Electronic Supplementary Material (ESI) for Environmental Science: Nano.

Supplement Information

The simultaneous purification of PM and NOx for diesel engine exhausts over a single 3DOM $Ce_{0.9-x}Fe_{0.1}Zr_xO_2$ catalyst

Ying Cheng, Jian Liu *, Zhen Zhao, Yuechang Wei, Weiyu Song, Chunming Xu

State Key Laboratory of Heavy Oil Processing, China University of Petroleum, Beijing 102249, China

* Corresponding author: Tel: 86-10-89732278. Fax: 86-10-69724721.

Email: liujian@cup.edu.cn

Number of Pages: 15

Number of Figures: 11

Number of Tables: 1

Table S1. Simultaneous NOx reduction and PM combustion over 3DOM catalysts (100 mg catalyst loosely mixed with 10 mg model PM; 1000 ppm NO, 1000 ppm NH_3, 3 % O_2 and balance N_2 at a gas hourly space velocity of 25000 h^{-1}).

Catalyst	**T_m[a] (°C)**	**$T_{full\ NO\ conversion}$[b] (°C)**
CeO_2	422	325-450
$Ce_{0.5}Zr_{0.5}O_2$	477	418-523
$Ce_{0.85}Fe_{0.1}Zr_{0.05}O_2$	415	365-503
$Ce_{0.7}Fe_{0.1}Zr_{0.2}O_2$	424	374-518
$Ce_{0.6}Fe_{0.1}Zr_{0.3}O_2$	449	380-517
$Ce_{0.5}Fe_{0.1}Zr_{0.4}O_2$	469	382-527

[a] Temperature of maximum CO_2 concentration;

[b] Temperature range where 100 % NO conversion is completed.

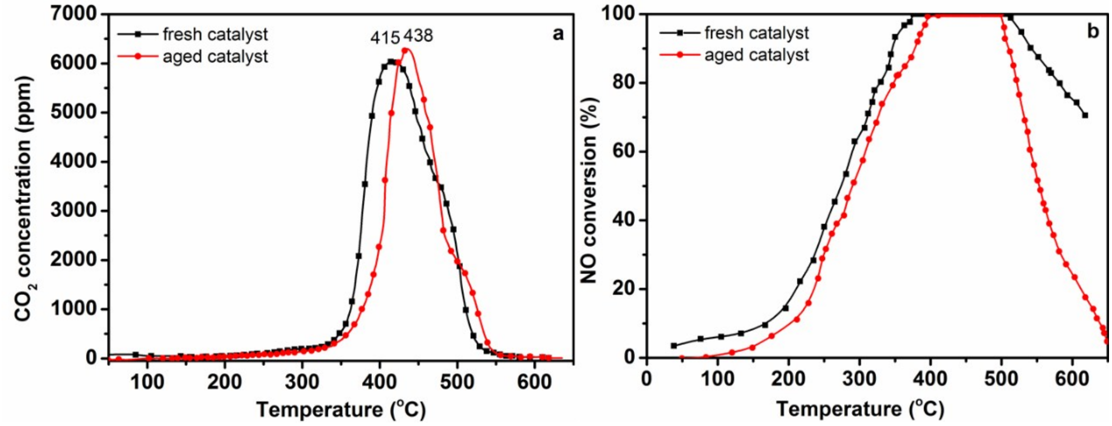

Figure S1. (a) CO_2 concentration and (b) NO conversion of 3DOM $Ce_{0.85}Fe_{0.1}Zr_{0.05}O_2$ catalysts fresh and aged at 800 °C for 5 h in air. After aging the catalyst was loosely mixed with Printex U model soot particles (reaction conditions: 1000 ppm NH_3, 1000 ppm NO, 3 % O_2 in N_2, model soot/catalyst mass ratio 0.1).

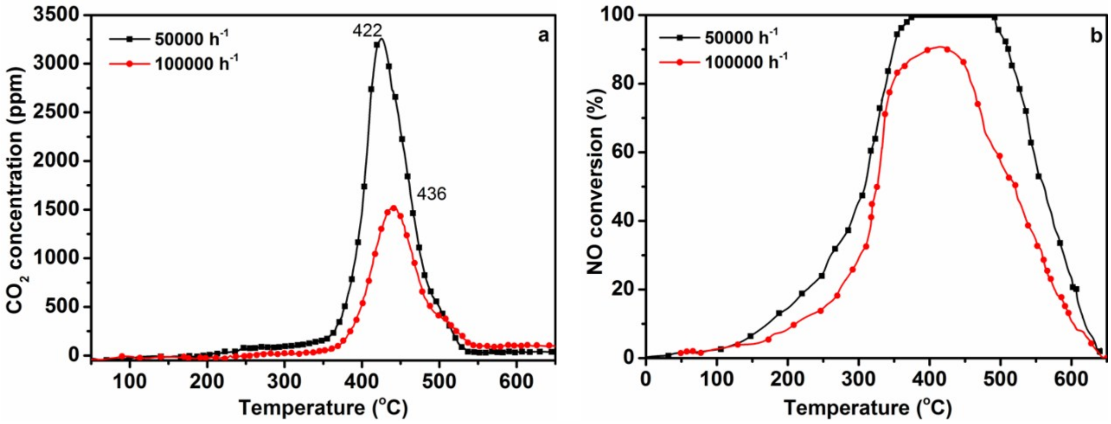

Figure S2. (a) CO_2 concentration and (b) NO conversion of 3DOM $Ce_{0.85}Fe_{0.1}Zr_{0.05}O_2$ catalysts loosely mixed with Printex U model soot particles at various GHSV (reaction conditions: 1000 ppm NH_3, 1000 ppm NO, 3 % O_2 in N_2, model soot/catalyst mass ratio 0.1)

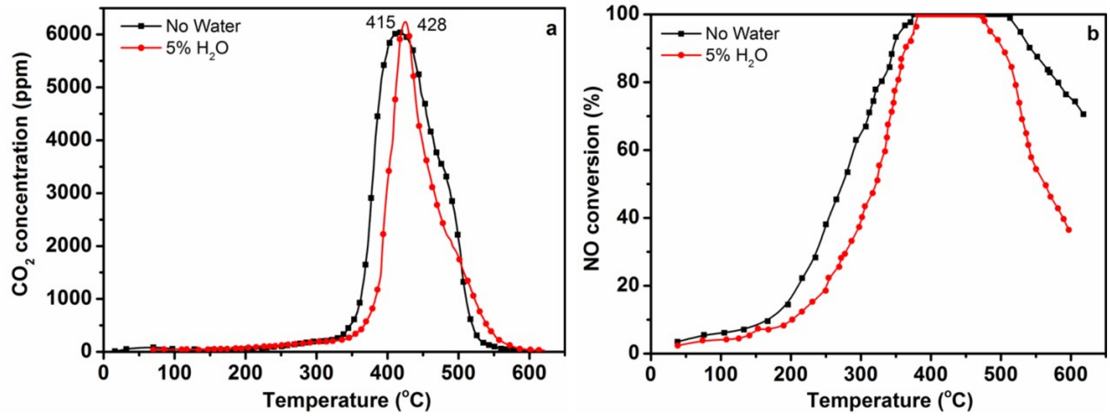

Figure S3. (a) CO_2 concentration and (b) NO conversion of 3DOM $Ce_{0.85}Fe_{0.1}Zr_{0.05}O_2$ catalysts (reaction conditions: GHSV = 25,000 h^{-1}, 1000 ppm NH_3, 1000 ppm NO, 3 % O_2 in N_2, model soot/catalyst mass ratio 0.1).

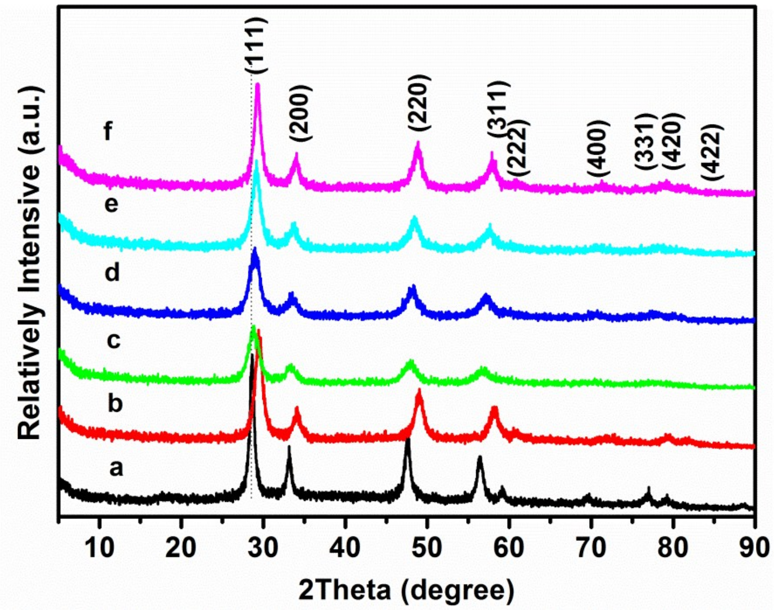

Figure S4. XRD patterns of 3DOM catalysts (a) CeO_2 (b) $Ce_{0.5}Zr_{0.5}O_2$ (c) $Ce_{0.85}Fe_{0.1}Zr_{0.05}O_2$ (d) $Ce_{0.7}$ $Fe_{0.1}Zr_{0.2}O_2$ (e) $Ce_{0.6}Fe_{0.1}Zr_{0.3}O_2$ (f) $Ce_{0.5}Fe_{0.1}Zr_{0.4}O_2$

3DOM $Ce_{0.9-x}Fe_{0.1}Zr_xO_2$ catalysts exhibit typical diffraction peaks belonging to CeO_2, giving an indication that the dopant does not change the cubic structure of the catalysts. 3DOM $Ce_{0.9-x}Fe_{0.1}Zr_xO_2$ catalysts shows a little lower XRD peak intensity as compared to the pure 3DOM CeO_2, which is due to the dopant decrease the crystallinity. Concurrently, it is noted that the diffraction peaks of 2θ show a slight shift to high angle as compared to the counterpart pure 3DOM CeO_2 catalyst. It is mainly due to that the ionic radius of Fe^{3+} or Zr^{4+} is smaller than that of Ce^{4+}. In addition, the diffraction peaks of 3DOM $Ce_{0.85}Fe_{0.1}Zr_{0.05}O_2$ are the weakest and broadest among all 3DOM $Ce_{0.9-x}Fe_{0.1}Zr_xO_2$ samples.

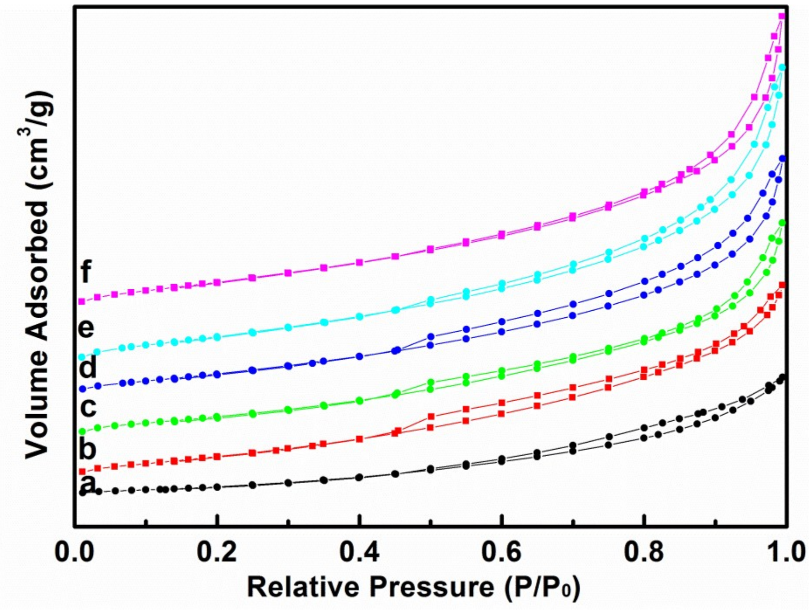

Figure S5. N_2 adsorption-desorption isotherms of 3DOM catalysts (a) CeO_2 (b) $Ce_{0.5}Zr_{0.5}O_2$ (c) $Ce_{0.85}Fe_{0.1}Zr_{0.05}O_2$ (d) $Ce_{0.7}Fe_{0.1}Zr_{0.2}O_2$ (e) $Ce_{0.6}Fe_{0.1}Zr_{0.3}O_2$ (f) $Ce_{0.5}Fe_{0.1}Zr_{0.4}O_2$

All the isotherms are in coordination with the type II isotherm accompanied with the H3 hysteresis loop in the relative high pressure (P/P_0) range and a nearly line correlation in the low pressure range. It is due to the unrestricted monolayer-multilayer adsorption. Whereas the appearance of the H3 hysteresis loop is an indication of the macroporous structure.[1,2] With regard to 3DOM $Ce_{0.9-x}Fe_{0.1}Zr_xO_2$ catalysts, it is noted that N_2 uptakes increase slightly in the middle relative pressure of 0.4-0.8, showing the presence of the mesopores. A sharply increases of the H3 hysteresis loop in the P/P_0 range of 0.8-1.0 of each sample is an indication of the macroporous structure.[3]

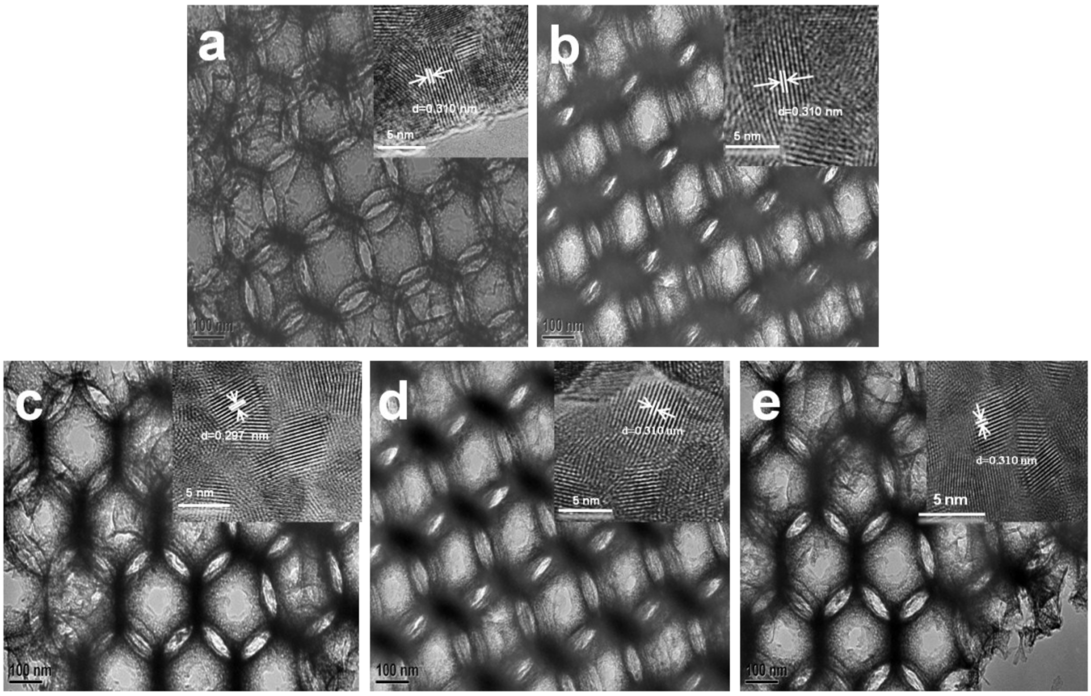

Figure S6. TEM images of 3DOM catalysts (a) CeO_2 (b) $Ce_{0.85}Fe_{0.1}Zr_{0.05}O_2$ (c) $Ce_{0.7}Fe_{0.1}Zr_{0.2}O_2$ (d) $Ce_{0.6}Fe_{0.1}Zr_{0.3}O_2$ (e) $Ce_{0.5}Fe_{0.1}Zr_{0.4}O_2$

Fig.S6 shows the representative TEM images of 3DOM $Ce_{0.9-x}Fe_{0.1}Zr_xO_2$ catalysts. It is clearly seen from Fig.S6 that all the samples possess a high-quality 3DOM architecture interconnected by the macrospores, which is in accordance with SEM observations. The ordered macrospore permits the reactant with large sizes to enter their inner pores, which can improve the contact efficiency between reactant and catalyst. Thus, the perfect macroporous structure provides the ideal reaction place to PM emitted from diesel engines. After making a statistic analysis of the sizes of the samples, the measured interplanar acing could be obtained. From TEM images of CeO_2 sample (Fig.S6a), the measured interplanar acing is 0.31 nm, which belongs to the (111) crystal plane of the standard card for CeO_2. For the other 3DOM $Ce_{0.9-x}Fe_{0.1}Zr_xO_2$ catalysts, no other interplanar acing except that CeO_2 can be detected, which is corresponding well to XRD and Raman results.

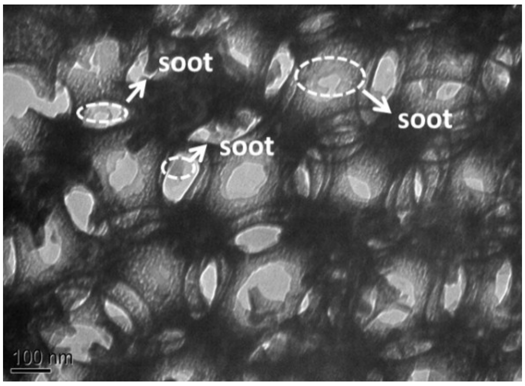

Figure S7. TEM images of 3DOM $Ce_{0.85}Fe_{0.1}Zr_{0.05}O_2$ catalyst mixed with Printex U after temperature programmed oxidation until 250 °C (reaction conditions: GHSV = 25,000 h^{-1}, 1000 ppm NH_3, 1000 ppm NO, 3 % O_2 in N_2, model soot/catalyst mass ratio 0.1).

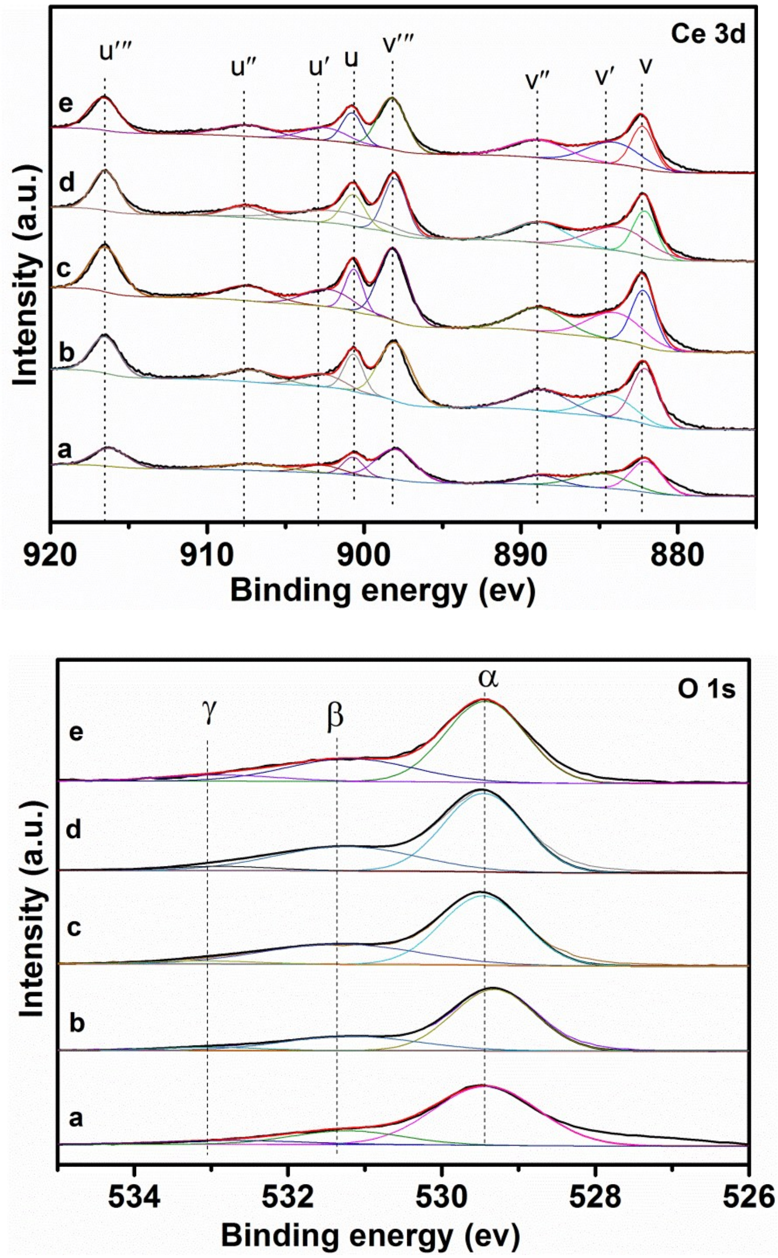

Figure S8. XPS curves of Ce3d, O1s for 3DOM catalysts (a) $Ce_{0.5}Zr_{0.5}O_2$ (b) $Ce_{0.85}Fe_{0.1}Zr_{0.05}O_2$ (c) $Ce_{0.7}Fe_{0.1}Zr_{0.2}O_2$ (d) $Ce_{0.6}Fe_{0.1}Zr_{0.3}O_2$ (e) $Ce_{0.5}Fe_{0.1}Zr_{0.4}O_2$

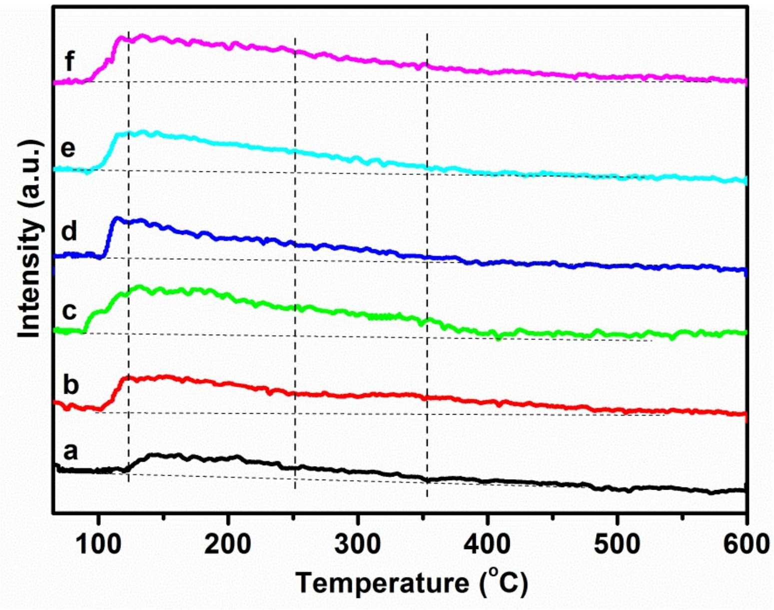

Figure S9. NH_3-TPD curves of 3DOM catalysts (a) CeO_2 (b) $Ce_{0.5}Zr_{0.5}O_2$ (c) $Ce_{0.85}Fe_{0.1}Zr_{0.05}O_2$ (d) $Ce_{0.7}Fe_{0.1}Zr_{0.2}O_2$ (e) $Ce_{0.6}Fe_{0.1}Zr_{0.3}O_2$ (f) $Ce_{0.5}Fe_{0.1}Zr_{0.4}O_2$

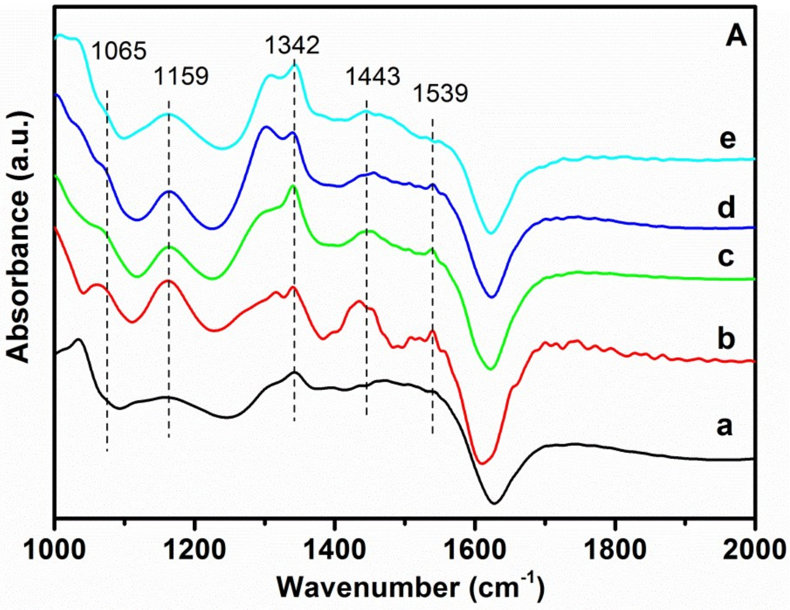

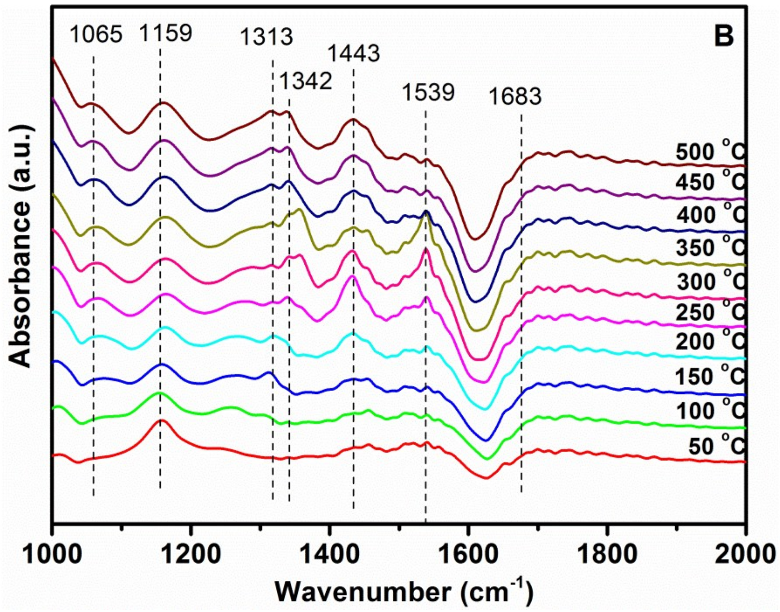

Figure S10. (A): In-situ DRIFT spectra of NH_3 desorption over 3DOM catalysts at 400 °C in the presence of 1000 ppm NH_3 (a) $Ce_{0.5}Zr_{0.5}O_2$ (b) $Ce_{0.85}Fe_{0.1}Zr_{0.05}O_2$ (c) $Ce_{0.7}Fe_{0.1}Zr_{0.2}O_2$ (d) $Ce_{0.6}Fe_{0.1}Zr_{0.3}O_2$ (e) $Ce_{0.5}Fe_{0.1}Zr_{0.4}O_2$ (B): In-situ DRIFT spectra of NH_3 desorption over 3DOM $Ce_{0.85}Fe_{0.1}Zr_{0.05}O_2$ catalysts in the presence of 1000 ppm NH_3 at different temperature

The in-situ DRIFT of NH_3 adsorption are detected to the change of acidity on the catalyst and presented in Fig.S10. The bands at 1065 and 1159 cm^{-1} are related to the coordinated NH_3 bound to Lewis acid sites, and the band at 1443 cm^{-1} is attributed to the NH^{4+} species on Brønsted acid. The bands at 1539 and 1342 cm^{-1} are also observed. The former is attributed to the asymmetric bending vibration of N–H bond in $–NH^{3+}$ group, which is generated from the decomposition of NH^{4+} chemisorbed on a Brønsted acid site. The latter is related to scissoring and wagging vibrations of $-NH_2$ species, which is formed by hydrogen abstraction from NH_3 coordinated to a Lewis acid site. For 3DOM $Ce_{0.9-x}Fe_{0.1}Zr_xO_2$ catalysts, the Lewis, Brønsted acids as well as $–NH^{3+}$ group and $-NH_2$ species can be detected, but for $Ce_{0.5}Zr_{0.5}O_2$ catalyst only the band ascribed to $-NH_2$ species are detected. The $–NH^{3+}$ group is easy to combine with NO to produce NO_3^-, which is beneficial for PM combustion. It indicates that after the dopant of Fe, Ce-Zr mixed oxides is prone to produce more $–NH^{3+}$ group.

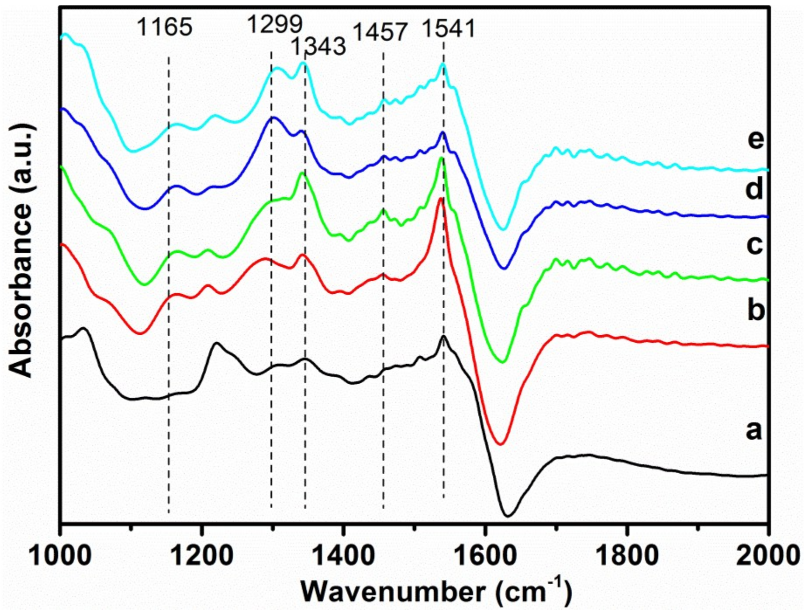

Figure S11. In-situ DRIFT spectra over 3DOM catalysts in a flowing of 1000 ppm NO+ 3% O_2 at 400 ^{o}C (a) $Ce_{0.5}Zr_{0.5}O_2$ (b) $Ce_{0.85}Fe_{0.1}Zr_{0.05}O_2$ (c) $Ce_{0.7}Fe_{0.1}Zr_{0.2}O_2$ (d) $Ce_{0.6}Fe_{0.1}Zr_{0.3}O_2$ (e) $Ce_{0.5}Fe_{0.1}Zr_{0.4}O_2$

Reference:

1 Y. Wang, H. Dai, J. Deng, Y. Liu, Z. Zhao, X. Li and H. Arandiyan, *Chem. Eng. J.*, 2013, **226**, 87-94.

2 X. Li, H. Dai, J. Deng, Y. Liu, S. Xie, Z. Zhao, Y. Wang, G. Guo and H. Arandiyan, *Chem. Eng. J.*, 2013, **228**, 965-975.

3 H. L. Fan, T. Sun, Y. P. Zhao, J. Shangguan and J. Y. Lin, *Environ. Sci. Technol,* 2013, **47**, 4859-4865.